DESIGN AND THEORETICAL PERFORMANCE PREDICTION OF HYDROGEN PEROXIDE HYBRID THRUSTER

Noor Muhammad Feizal B Muhalim, Subramaniam Krishnan,
Mohammad Nazri bin Mohd. Jaafar, and Wan Khairuddin bin Wan Ali
Department of Aeronautical Engineering, Faculty of Mechanical Engineering
Universiti Teknologi Malaysia, 81310 Skudai, Malaysia
e-mail: krishnan@fkm.utm.my

[Presented at the Conference on Aerospace Technology of the XXI Century (AEROTECH III – 2009),18-19 November 2009, Kuala Lumpur]

ABSTRACT
A design procedure to realize a hybrid rocket engine that uses hydrogen peroxide as the oxidizer and a solid polymer as the fuel is presented. In the design procedure, the products of decomposition and of combustion at different stations are calculated by linking a standard complex chemical-equilibrium program of NASA. For the designed basic-configuration, applying the mass conservation principle, theoretical performance results are presented with propellant-tank pressure and grain port length as parameters.

Keywords: hybrid rocket/ hydrogen peroxide/ performance prediction

1. INTRODUCTION

In recent years, there has been a renewed interest in the use of hydrogen peroxide (H_2O_2) as an oxidizer in bipropellant liquid rocket engines as well as in hybrid rocket engines [1-4]. This renewed interest is because of the growing importance in using propellants of low toxicity and enhanced versatility. The use of H_2O_2 in rocket propulsion offers the versatility of operating the engine on a dual mode, namely, a bipropellant mode for a large thrust requirement (either as a bipropellant liquid engine or as a hybrid rocket engine) and a monopropellant mode for a small thrust application. A propulsion unit without a requirement for a separate ignition unit offers a higher system-reliability. H_2O_2 decomposes into a mixture of superheated steam and oxygen to a temperature of around 1000K. This leads to automatic ignition either with a liquid fuel in a bipropellant engine or with a solid fuel in a hybrid-rocket engine. Thus, the versatility with the additional advantage of automatic ignition makes the “green” H_2O_2 an attractive oxidizer.

In light of the current interest in H_2O_2 propulsion, the present study draws out a design methodology for the hybrid engine. A small hybrid rocket engine with gas pressurization is taken for the study and in line with the convention, let us hereafter term the engine as thruster.

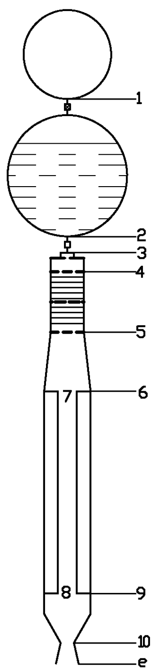

Fig. 1 Gas pressurized hydrogen peroxide hybrid rocket thruster.

1.1 Hydrogen Peroxide Hybrid Rocket Thruster

The sketch along with reference station-numbers of a gas pressurized hybrid rocket thruster is given in Fig. 1. The three major components of the thruster are (i) the high-pressure neutral-gas tank with a pressure of p_{01}, (ii) the high concentration H_2O_2 propellant-tank maintained at a pressure p_{02}, and (iii) the propulsion unit comprising of injector, catalyst pack, solid fuel grain, and nozzle. As H_2O_2 is being consumed, downstream of the neutral-gas tank is a pressure regulator that maintains the desired pressure p_{02} in the propellant tank. Across the pressure regulator, there is a requirement of a minimum pressure difference between p_{01} and p_{02}. Downstream of the propellant tank is the normally closed on-off solenoid valve that introduces a pressure loss when kept opened. The valve allows H_2O_2 to be injected at p_{03} into the pre-chamber of pressure p_{04}. For a good atomization as well as to effectively de-link the feed system from the thruster a sufficient pressure drop ($\Delta p_{0inj} = p_{03} - p_{04}$) is required across the injector orifice. As the injected H_2O_2 flows through the catalyst pack, it decomposes into an oxidant mixture essentially of superheated steam and oxygen. Depending on the value of mass flux of H_2O_2 through the catalyst pack there is a pressure loss ($\Delta p_{0CP} = p_{04} - p_{05}$) resulting in a pressure p_{05} at the outlet of the catalyst pack.

Normally, in order to accommodate the fuel grain, there is an increase in flow area from the outlet section of the catalyst pack, station 5 of Fig. 1. This introduces a pressure loss from p_{05} to p_{07}. The oxidant mixture of temperature around 1000K enters the fuel grain port. The fuel grain automatically ignites because of this high temperature.

In the fuel grain-port, the mass addition due to the regressing solid fuel and its combustion with the oxidant cause a pressure loss leading to a reduced pressure p_{08} at the outlet of the fuel grain port. The sudden area variation from the outlet of the grain port to the plenum brings about further pressure loss resulting in the plenum pressure of p_{09}. After accounting for the nozzle pressure loss through a suitable value for the nozzle pressure-loss-factor, the pressure at the nozzle throat is p_{010}.

During the thruster operation, the mass flow rate ejected through the nozzle throat at p_{010} should be equal to the total mass flow rate of the combustion products exiting the grain port. This mass-conservation condition forms the fundamental basis for predicting the entire thruster-performance comprising of ignition transient, equilibrium operation, and tail-off transient.

2. DESIGN

The thruster is chosen to deliver about 200N thrust with a thrusting time of 5s at standard sea level. For the present study polymethyl methacrylate (PMMA; $C_5H_8O_2$) is adopted as the solid fuel.

Generally the maximum chamber pressure employed for H_2O_2 systems is less than 3MPa. Therefore with the pre-chamber pressure p_{04} of 3MPa, and allowing an injector pressure drop of about 0.7 MPa and some pressure loss across the on-off solenoid valve, the propellant tank pressure p_{02} is kept at 3.75MPa. As previously indicated, allowing a minimum pressure difference of 1MPa across the pressure regulating valve, the possible minimum pressure in the neutral gas tank $p_{01_{min}}$ = 4.75MPa.

For the decomposition of H_2O_2, there are two important parameters for the design of a screen bed catalyst pack: (i) the average mass flux through the bed ($\dot{m}_o / A_{CP}$, the so called bed-loading) and (ii) the average residence time. Among the screen bed systems, pure silver screen is often found to be employed. In proven beds of silver screen, adopted values of mass-flux vary from 117- to 280-kg/m^2-s [5-8] and average residence time in the catalyst bed varies from 0.7ms to 2 ms [6-9]. The pressure drop across the catalyst pack Δp_{0CP} is found to be a linear function of the mass flux $\dot{m}_o / A_{CP}$ [5].

$$\Delta p_{0CP} = K_1 \left(\dot{m}_o / A_{CP} \right) \qquad (1)$$

Accounting for the pressure drop across the catalyst pack for an average mass flux of 200 kg/m^2-s, the estimated average pressure across the catalyst pack = 2.45MPa. Using the CEC71 program of NASA [10], the decomposition characteristics of H_2O_2 for this pressure are calculated and given in Table 1. The decomposed products are essentially H_2O and O_2.

Since the thruster under consideration has to decompose H_2O_2 through a catalyst pack a conservative value of 0.90 is assumed for the c^* efficiency, η_{c^*}. Thus the estimated experimental decomposition temperature = 834.3K. As a conservative estimate, the pressure at the inlet to the grain port p_{07} can be taken as equal to p_{06}, which is calculated by assuming a suitable diffuser isentropic-efficiency η_d from the station 5 to 6.

Table 1 Characteristics of H_2O_2 decomposition products

Details	Values
H_2O_2 concentration (specified)	0.9
Average pressure across catalyst pack (specified) (MPa)	2.45
Adiabatic decomposition temperature (K)	1030
Molar mass (kg/kg-mole)	22.105
Ratio of specific heats	1.2648
H_2O mole fraction	0.70757
O_2 mole fraction	0.29243

In rocket propulsion systems, the maximum specific impulse is obtained for fuel rich condition. Just for sizing the thruster, however, the equivalence ratio of 1 is adopted. Using again the CEC71 program [10], the rocket performance is calculated for the equivalence ratio of 1 at the average pressure of 2MPa, which is the estimated pressure after accounting for the losses through diffusion (station 5 – 7), and mass addition and combustion (station 7 – 8). The grain-port entry temperature of the oxidant mixture is kept at the previously estimated temperature of 834.3K. The results of the calculation are given in Table 2.

For an assumed η_{c^*} of 0.9 in the grain port, the estimated c^*_{expt} = 1362.6 m/s. With the nozzle flow efficiency of 0.95, the corrected thrust coefficient for operation in standard sea level condition C_F = 1.332. Thus the corrected specific impulse = 1814 N-s/kg. With this specific impulse, the 200N thruster requires a total-propellant flow of 0.1103 kg/s. For the specified equivalence ratio of 1, the oxidizer fuel ratio = 4.5335 (Table 2). Hence, the required H_2O_2-oxidizer flow rate = 0.0904 kg/s and the fuel flow rate = 0.0199 kg/s.

Noting

$$F = C_F \, p_{0n} A_t \tag{2}$$

the throat diameter is calculated and rounded to 0.010m. Assuming an initial port-to-throat area-ratio of 2, the rounded initial-diameter of the grain port = 14mm and this corresponds to the maximum oxidizer mass flux through the grain port as 587 kg/m^2-s that is acceptable. Adopting the semi-empirical equation [11] for fuel regression rate,

$$\dot{r}_F = K_2 G_o^{n_1} d_f^{-n_2} \tag{3}$$

$\dot{r}_F$ = 2.4mm/s. Therefore, for the 5s operation the maximum outer diameter of the fuel grain is to be around 0.038 m.

Table 2 Characteristics of H_2O_2-PMMA thruster

Details	Values
Heat of formation of H_2O at 834.3K (MJ/kg-mole)	222.479
Heat of formation of O_2 at 834.3K (MJ/kg-mole)	16.998
Heat of formation of PMMA - $C_5H_8O_2$ (specified) (MJ/kg-mole)	379.664
Average chamber pressure (specified) (MPa)	2
Nozzle area ratio (specified) ε	2.94
Equivalence ratio (specified) ϕ	1
Oxidizer fuel ratio O/F	4.5335
Adiabatic flame temperature (K) T_0'	2632
Molar mass of combustion products (kg/kg-mole) $\overline{m}$	22.97
Ratio of specific heats γ	1.1830
Nozzle pressure ratio p_{010}/p_e	14.605
Characteristic velocity (m/s) c^*_{theo}	1514
Characteristic thrust coefficient C_F^0	1.35

For the fuel flow rate of 0.0199 kg/s and with the fuel regression rate of 0.0024 m/s, the length of the fuel grain port = 0.160 m.

For the assumed 200 kg/m^2-s mass flux of H_2O_2 and the calculated oxidizer mass flow rate of 0.0904 kg/s through the catalyst pack, the rounded diameter of the catalyst pack = 0.025m. For the conservatively chosen long residence-time of 2 ms, the rounded length of the catalyst pack = 0.055m.

With an assumed value of 0.8 for the coefficient of discharge $C_{d_{inj}}$ and the specified pressure drop across the injector at 0.7MPa, the injector orifice diameter = 1.8 mm.

For the H_2O_2 flow rate of 0.0904 kg/s for 5 s, with suitable allowance for ullage, the propellant tank volume is calculated to be 400 ml. Next we have to consider the tank volume of pressurizing neutral-gas. Nitrogen is chosen as the pressurizing gas. Assuming adiabatic process (the energy of the pressurizing gas is constant from the initial to final conditions) and ideal gas condition, and neglecting the initial mass of the pressurizing gas in the propellant tank and piping, a simple procedure may be followed to fix the tank volume of the pressurizing gas [12,13]. Under these assumptions, for the initial and final pressures in the pressurizing-gas tank, p_{gi} = 20 MPa and p_{gf} = 5MPa, the volume of the pressurizing neutral gas is calculated as 150 ml.

The sized hybrid thruster is shown in Fig. 1. The detailed numerical calculations are given in the Appendix. Although the thruster is sized for the specified values, a procedure for theoretical performance prediction can be developed under the mass conservation condition, namely, the rate of mass accumulation in the rocket chamber should be equal to the entering mass flow rates by way of H_2O_2 injection and the fuel regression rate, and the exiting mass flow rate though the choked nozzle. In this procedure, the variations of the operational parameters, namely propellant tank pressure p_{02} and atmospheric pressure p_a are possible. Also possible are the variations of the design parameters, namely, injector orifice diameter d_{inj}, initial diameter of grain port d_{fi}, fuel-grain length l_f, and nozzle throat diameter d_{10}. All the three phases of thruster operation, namely ignition transient, equilibrium operation, and tail-off transient can be considered in the procedure.

3. RESULTS AND DISCUSSION

A computer-code was written to predict the performance of the H_2O_2 hybrid thruster for various parametric values. The dimensions of the basic design-configuration, and the figures of merit and other values adopted are given in Table 3. Performances predicted for two different pressures in the propellant tank is given in Fig. 2. Similarly effects of variations of other parameters can be obtained. The predicted performance is in line with typical rocket engine behavior: (i) longer tailoff, and higher values of thrust, specific impulse and hence total impulse for lower atmospheric pressure, (ii) shorter thrusting time and higher thrust for higher propellant-tank pressure (Fig. 2), (iii) lower chamber pressure, longer thrusting time with lower thrust, and lower specific impulse for smaller injector orifice, (iv) longer thrusting time for smaller initial grain-port diameter, (v) higher chamber pressure and longer thrusting time with smaller thrust for smaller nozzle throat-diameter. The results of the calculations to find the grain-port length for the maximum specific impulse under vacuum condition are summarized in Fig. 3.

Table 3 Basic design configuration and other adopted values

Dimensions		Figures of merit	Other values
d_{inj} = 1.8 mm	d_{fo} = 20 mm	$C_{d_{inj}}$ = 0.8	α = 0.9
d_{CP} = 25 mm	d_9 = 35 mm	η_{c^*} = 0.9	Δp_{0oo} = 0.2MPa
l_{CP} = 55 mm	d_{10} = 10 mm	η_d = 0.9	K_1 = 6.37x10^{-5}
d_5 = 21 mm	ε = 2.939	r_n = 0.98	n_1 = 0.41
d_6 = 30 mm		η_F = 0.98	n_2 = 0.24
d_{fi} = 14 mm			K_2 = 3894

Although various figures of merit and other constants have been specified as given in Table 3 and elsewhere, adopting or finding their correct values forms the part of the development of a specific thruster.

4. CONCLUSIONS

A design procedure for the hydrogen peroxide hybrid thruster has been explained for the first cut sizing. The complex chemical equilibrium composition for the hydrogen peroxide decomposition and for the subsequent combustion in the fuel grain port, and the rocket performance for the nozzle entry pressure are all calculated by linking a widely adopted NASA code. It is important to model the thruster to predict its performance under different design and operational conditions. While the prediction under former condition helps in arriving at the near-exact sizing of the thruster before fabrication, that under the latter, by predicting the bench mark performance and comparing the same with the hot test results, helps in the development of the thruster to the final configuration. The hybrid thruster performance calculated and presented here are in line with the typical trends.

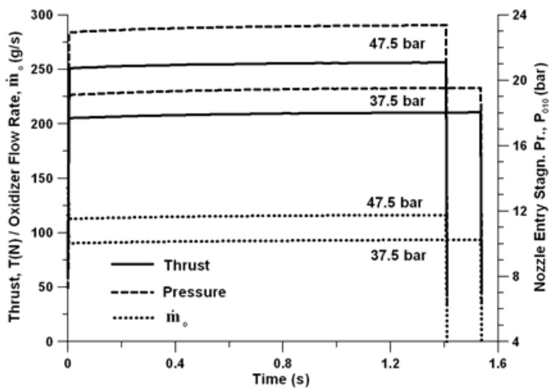

Fig. 2. Performance prediction for different pressures in H_2O_2 propellant tank.

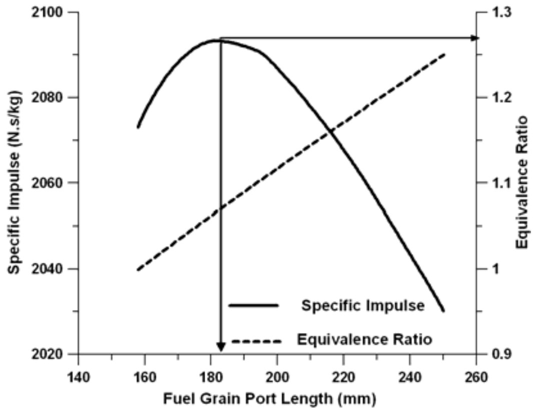

Fig. 6 Variation of vacuum specific impulse and equivalence ratio with fuel grain port length.

5. APPENDIX

Pure H_2O_2 has the density of 1442.5 kg/m^3. At the mass concentration of α, the density of H_2O_2 – water mixture,

$$\rho_{\alpha o} = \frac{\rho_{H_2O_2}\rho_{H_2O}}{\alpha\rho_{H_2O} + (1-\alpha)\rho_{H_2O_2}} \qquad \text{(A. 1)}$$

Therefore at α = 0.9, $\rho_{0.9o} = 1381.37\, kg/m^3$. The theoretical characteristic velocity c^*_{theo} is defined as

$$c^*_{theo} = \frac{\sqrt{RT_0}}{\Gamma} \quad where \quad \Gamma = \sqrt{\gamma}\left(\frac{2}{\gamma+1}\right)^{\frac{(\gamma+1)}{2(\gamma-1)}} \qquad \text{(A. 2)}$$

The c^* efficiency, $\eta_{c^*} \equiv c^*_{expt}/c^*_{theo}$. Assuming η_{c^*} = 0.9 and noting that the adiabatic decomposition temperature of 0.9 concentration H_2O_2 is calculated as 1030K (Table 1), the estimated experimental decomposition temperature T_{04} = 834.3K.

For the combustion with equivalence ratio = 1 in the PMMA grain port, the calculated c^*_{theo} = 1514 m/s (Table 2). Again assuming η_{c^*} = 0.9 the estimated $c^*_{expt} = \eta_{c^*} \times c^*_{theo} = 1362.6$ m/s. Specified are the nozzle quality factor η_F = 0.95, nozzle area ratio ε = 2.94 , nozzle throat stagnation pressure p_{0n} = 2MPa, and atmospheric pressure p_a = 0.101325 MPa. With the calculated values of C_F^0 = 1.35 and p_{0n}/p_e = 14.605 (Table 2), the estimated experimental thrust coefficient $C_{F_{expt}} = \eta_F C_{F_{theo}}$ = 1.3322. The specific impulse $I_{sp} \equiv F/\dot{m}_p = c^* C_F$. Therefore the estimated experimental specific impulse, $I_{sp_{expt}} = c^*_{expt} C_{F_{expt}} = 1815.3$ N-s/kg. To produce a thrust of 200N the propellant flow rate,

$$\dot{m}_p = \frac{F}{I_{sp_{expt}}} = 0.1102 kg/s \qquad \text{(A. 3)}$$

Noting that for the equivalence ratio of 1, the calculated oxidizer: fuel ratio, O/F = 4.5335 (Table 2). The fuel flow rate is given by

$$\dot{m}_F = \frac{\dot{m}_p}{1+O/F} \qquad \text{(A. 4)}$$

Hence, $\dot{m}_F$ = 0.0199 kg/s. And, $\dot{m}_o = \dot{m}_p - \dot{m}_F$ = 0.0903 kg/s. The thrust $F = C_F p_{0n} A_{10}$. For the desired thrust of 200N, the nozzle-throat area is calculated as,

$$A_{10} = \frac{F}{C_{F_{expt}} p_{0n}} = 7.5064 \times 10^{-5} m^2 \qquad \text{(A. 5)}$$

For this throat area the rounded throat-diameter = 10mm. Assuming an initial port-to-throat ratio, $A_{fi}/A_t = 2$, the initial rounded-diameter of the grain port = 14mm. For this diameter the oxidizer mass flux, $G_o = \dot{m}_o/A_{fi}$ = 586.6 kg/m^2-s. The regression rate for PMMA is assumed as [11],

$$\dot{r}_F = 6.37 \times 10^{-5} G_o^{0.41} D_p^{-0.24} m/s \qquad \text{(A. 6)}$$

Therefore the regression rate of the fuel, $\dot{r}_F = 2.42 \times 10^{-3} m/s$. Noting that the density of the PMMA fuel = 1181.6 kg/m^3, the length of the fuel grain can be calculated as,

$$l_f = \frac{\dot{m}_F}{\pi d_{fi} \rho_F \dot{r}_F} = 0.158 m \qquad \text{(A. 7)}$$

Assuming an average mass flux of 200 kg/m^2-s through the catalyst pack A_{CP} = 4.515x10^{-4} m^2. The corresponding rounded diameter of the catalyst pack = 25mm. The average velocity through the catalyst pack,

$$u_{CP} = \frac{\dot{m}_o}{\rho_{CP} A_{CP}} = 23.56 m/s \qquad \text{(A. 8)}$$

Assuming a residence time of Δt_{CP} of 2 ms, the length of the catalyst pack $l_{CP} = \Delta t_{CP} \times u_{CP} = 0.047$m. As there are perforated plates of stainless steel interposed in the catalyst pack to avoid tunneling effect, the total length of the catalyst pack is kept at 55mm.

To effectively de-link the feed system from the engine, generally about 0.7MPa or 10 percent of the chamber pressure, whichever is higher, is provided at the propellant injector. Therefore, a pressure drop of 0.7MPa is provided for the propellant injection. For the mass flow-rate of H_2O_2 = 0.0903 kg/s, assuming the coefficient of discharge for the orifice as *0.8*, the orifice diameter can be calculated from,

$$\dot{m}_o = C_{d_{inj}} \left(\frac{\pi d_{inj}^2}{4} \right) \sqrt{2 \Delta p_{0inj} \rho_{\alpha o}} \qquad \text{(A. 9)}$$

and it is rounded to 1.8mm.

For the H_2O_2 flow rate of 0.0903 kg/s for 5 s, with the density $\rho_{0.9o}$ = 1381.37 kg/m^3, the total volume of the H_2O_2 propellant, $V_{0.9o}$ = 3.268x10^{-4} m^3. In the propellant tank, a suitable additional volume for the ullage has to be provided. Furthermore, the provision of elaborate swirl-spoilers at the drain port of the propellant tank is not envisaged. Considering all these, giving a 20 percent increase for ullage and excess propellant, the propellant-tank volume, $V_{0.9o,tank}$ is rounded to 400ml.

Nitrogen is to be used as the pressurizing gas. Assuming adiabatic process and ideal gas condition, and neglecting the initial mass of the pressurizing gas in the propellant tank and piping, the volume of the pressurizing neutral gas can be calculated for the specified initial and final pressures in the pressurizing-gas tank, p_{gi} = 20

MPa and p_{gf} = 5MPa [12,13]. The tank volume of the pressurizing neutral gas

$$V_{g,tank} = V_{\alpha o,tank} \frac{p_{02}}{p_{gi}} \left(\frac{\gamma_g}{1 - p_{gf} / p_{gi}} \right) = 1.4 \times 10^{-4} m^3 \qquad \text{(A. 10)}$$

A rounded tank-volume of 150ml is chosen for the pressurizing neutral gas. The sketch of the sized hybrid rocket thruster is given in Fig. 1.

6. REFERENCES

1. N. Tsujikado, M. Koshimae, R. Ishikawa, K. Kitahara, A. Ishihara, Y. Sakai, and K. Konishi, An Application of Commercial Grade Hydrogen Peroxide for Hybrid/Liquid Rocket Engine, AIAA paper 2002-3573, 2002.
2. E. Wernimont and M. Ventura, Catalyst Bed Testing for Development of a 98% Hydrogen Peroxide Procurement Specification, AIAA paper 2002-3852, 2002.
3. T. R. Beutien, S. D. Heister, J. J. Rusek, and S. Meyer, Cordierite-Based Catalytic Beds for 98% Hydrogen Peroxide, AIAA paper 2002-3853, 2002.
4. W. J. Helms, J. S. Mok, J. C. Sisco, and W. E. Anderson, Decomposition and Vaporization Studies of Hydrogen Peroxide, AIAA paper 2002-4028, 2002.
5. E. J. Wernimont and P. Mullens, Capabilities of Hydrogen Peroxide Catalyst Beds, AIAA Paper 2000-3555, 2000.
6. C. M. Willis, The Effect of Catalyst-Bed Arrangement on Thrust Buildup and Decay Time for a 90% Hydrogen Peroxide Control Rocket, NASA TND–516, 1960.
7. J. P. Wanheim, P. S. Ross, and R. L. DeWitt, Effect of Propellant and Catalyst Bed Temperatures on Thrust Buildup in Several Hydrogen Peroxide Reaction Control Rockets, NASA TND-480, 1960.
8. J. F. Runckel, C. M. Willis, and L. B. Salters Jr., Investigation of Catalyst Beds for 98% Concentration Hydrogen Peroxide, NASA TND-1808, 1963.
9. J. E. Love and W. H. Stillwell, The Hydrogen Peroxide Rocket Reaction-Control System, NASA TN D-185, 1959.
10 S. Gordon and B. J. McBride, Computer Program for Calculation of Complex Chemical Equilibrium Compositions, Rocket Performance, Incident and Reflected Shocks, and Chapman-Jouguet Detonations, NASA SP-273, 1971.
11. Philmon George, S. Krishnan, P. M. Varkey, M. Ravindran, and R. Lalitha, Fuel Regression Rate Enhancement Studies in HTPB/GOX Hybrid Rocket Motors, Vol. 17 (1), pp. 35-42, *Journal of Propulsion and Power,* 2001.
12. M. Barrere, A. Jaumotte, B. F. De Veubeke, and J. Vandenkerckhove, *Rocket Propulsion*, pp. 474-480, Elsevier Publishing Company, Amsterdam, 1960.
13. G. P. Sutton, and O. Biblarz, *Rocket Propulsion Elements,* 7th Edition, pp. 220-221, John Wiley & Sons, Inc., New York, 2001.